Journal of Molecular Structure 1106 (2016) 59–63

Contents lists available at ScienceDirect

Journal of Molecular Structure

journal homepage: http://www.elsevier.com/locate/molstruc

Crystal structure and band gap studies of sodalite: experimental and calculated results

Lijun Pan [a, *], Wanchao Liu [b], Weiguang Chen [a], Kun Yan [b], Huizhi Yang [c], Jia Yu [d, *]

[a] College of Physics and Electronic Engineering, Zhengzhou Normal University, Zhengzhou, 450044, China
[b] Zhengzhou Research Institute of CHALCO, Zhengzhou, 450041, China
[c] College of Science, Henan Institute of Engineering, Zhengzhou, 451191, China
[d] Center for Clean Energy and Quantum Structures, School of Physics and Engineering, Zhengzhou University, Zhengzhou, 450052, China

ARTICLE INFO

Article history:
Received 11 July 2015
Received in revised form
8 October 2015
Accepted 19 October 2015
Available online 22 October 2015

Keywords:
Sodalite
Crystal structure
Electrical properties
Density functional theory

ABSTRACT

In this paper, we investigated the crystal structural properties of sodalite sample by X-ray diffraction and the band gap studies by means of UV–Vis absorption spectroscopy, and compared with the calculated results using density functional theory. The results of X-ray diffraction suggests that the chemical formula should be $Na_8(AlSiO_6)_4(OH)_2\cdot 2(H_2O)$. The optimized lattice parameter is found to be larger 0.45% than experimental value and the calculations demonstrated the structural details of the hydrogen bond located in sodalite cage. The hydrogen bond formed by water molecule and hydroxyl is implied from charge distribution analysis. As the rotation angle of O–O lines in hydrogen bond is 51.8°, the structure should be of the lowest energy. The optical band gap is measured to be 4.5–4.7 eV experimentally, while, the calculated value is 4.16 eV which is attributed to the localized state below Fermi level formed by the hydrogen bonds. Our results are favorable for the understanding the role of sodalite in silicate mud and contribute to further disposals and treatments.

1. Introduction

Sodalites are a series of crystalline materials with the common feature of polyhedral cages (β-cages) usually formed by a network of alternating and corner-sharing SiO_4 and AlO_4 tetrahedrons. The naturally mineral sodalite $Na_8Al_6Si_6O_{24}Cl_2$ is defined as each cage including four sodium cations at sites close to the six-ring opening and anions in the center [1]. As a porous framework structure, β-cage may enclathrate various anions, cations and molecules which is regarded as a model compound for relevant zeolites A, X and Y [2]. The sodalite range covers $Na_8Al_6Si_6O_{24}(OH)_2\cdot 2H_2O$ [3–5], anhydrous $Na_8[AlSiO_4]_6(OH)_2$ [6], Na-doped dehydrated sodalite $Na_8[AlSiO_4]_6$ [7–9], Aluminate sodalite $Sr_8[Al_{12}O_{24}](CrO_4)_2$ [10], silica sodalite [11], $Si_{12}O_{24}$ [9,12,13], CH_2 and NH doped $Si_{12}O_{24}$ [14], $Si_{12}O_{24}\cdot 2C_2H_4(OH)_2$ [15] and so on. Precisely, for $Na_8Al_6Si_6O_{24}(OH)_2\cdot 2H_2O$, the $(O_2H_3)^-$ group is found experimentally with the strong central hydrogen bond and O–O distance about 2.44 Å [3] or 2.3 Å [4] which has point symmetry. On the whole, the hydrosodalites are expressed as $Na_{6+x}(SiAlO_4)_6(OH)_x\cdot nH_2O$, and five phases may form by altering the number of hydroxyls or water molecules [5].

The sodalites have structural distortions to some extent by introducing certain ions. Such a s the $Na_8[Al_6Si_6O_{24}]SO_4\cdot H_2O$ [16], the $Na_8(AlSiO_4)_6(ReO_4)_2$ [17], or binary substitution including of $(ReO_4)^-$ [18], $Na_8[A1SiO_4]_6(NO_3)_2$ [19] and $Na_8[AlSiO_4]_6(BH)_2$ [20,21]. Moreover, as the heavy metal cations may be introduced through covalent bonds with the aluminosilicate framework, the structures should belong to the low cubic space group in studies [22–24]. The detailed study demonstrated that O–H bond also has ability of causing the local distortion of the framework and affecting the vibrational spectra [25].

The structures of the sodalites vary due to the different combination of the cations, anions and molecules in sodalite framework not only to preserve the structural stability and electrically neutral but also to induce the electronic properties variety of the sodalites. Blake et al. investigated the sodalite $Na_8Al_6Si_6O_{24}$ and found to be metallic which may be opposite of the infrared absorption spectrum results with the maximum value of 2.5 eV [7]. As the F center forms at center of the cage, the sodalite $(Na/K)_8(AlSiO4)_6$ may absorb light with the energy around 1 eV and above [26]. Which is in agreement with the calculation [7,9,27]. Al-substitution and

* Corresponding author.
E-mail addresses: lijunpan515@163.com (L. Pan), jiayu@zzu.edu.cn (J. Yu).

http://dx.doi.org/10.1016/j.molstruc.2015.10.045
0022-2860/

cation compensation are showed to have effects on the energy bands at the upper valence band edge [12]. The photon band gap of $Na_8[GaSiO_4]_6(NO_2)_2$, $Na_{3.12}K_{4.88}[GaSiO_4]_6(NO_2)_2$ and $Na_{2.02}Ag_{5.98}[GaSiO_4]_6(NO_2)_2$ measured by UV-DRS is 3.48 eV, 3.46 eV and 3.26 eV, respectively [28]. The filling III–V clusters in sodalite is calculated to lower the band gap of natural sodalite, 4.4 eV [29] and the band gap may grow for increasing cluster size [30]. Similarly, Si clusters are found to lower the band gap of $Si_{12}O_{24}$ [13]. Using first principles, the neutral sodalite $Si_6Al_6O_{24}$ is found to be metallic, and the natural sodalite $Na_8Si_6Al_6O_{24}Cl_2$, the anhydrous sodalite $Na_6Si_6Al_6O_{24}$ has the band gap of 4.39 eV, 3.78 eV, respectively, which are in good agreement with experimental data [31]. While the recently calculation showed that natural sodalite $Na_8Si_6Al_6O_{24}Cl_2$ has the band gap value of 5.0 eV [32].

As mentioned above, the existing researches mainly focused on the component and performance characterization by filling "guest" ions and molecules. However, the accurate calculations under the frame of the first principles are rare. In this paper, we investigated and characterized the sample from the silicate mud and calculated its structural and electronic properties using the first principles for sake of understanding the silicate mud and favorable of further processing.

2. Methods

The samples were prepared and provided by Zhengzhou Research Institute of CHALCO. The X-Ray Powder Diffraction (XRD) patterns were obtained with a Bruker D8 instrument using Cu K_α radiation at 40 mA and 40 KV. The samples were characterized from 3° to 90° 2θ at a scanning speed of 1° 2θ min^{-1} with a scan step of 0.05° 2θ. The absorption and reflection spectroscopy were performed on an Ultraviolet–visible spectroscopy (UV–Vis) (Shimadzu 3600) with the response time 1 s, a 2 nm slit width to establish the type of band-to-band transition.

All calculations herein were performed with the Vienna *ab initio* simulation Package (VASP) [33,34] based on density functional theory. Briefly, we applied the polarized projector augmented wave (PAW), Perdew-Burke-Ernzerhof (PBE) generalized gradient approximation (GGA) [35,36] and periodic boundary conditions with the energy cutoff 400 eV. We set the energy and the force convergence criterion on each atom to be 0.0001 eV, 0.01 eV/Å, respectively. A Monkhorst-pack grid [37] $5 \times 5 \times 5$ for sampling the Brillouin zone and the stress tensor calculations were selected. The initial structure is constructed according to results of XRD, and then the lattice parameters of the final calculated results are checked to ensure that the total energies are reliable. Finally, the band structure calculations are carried out and compared with the results of UV–Vis.

3. Results and discussion

3.1. The experimental studies of the sample

The X-ray power patterns of the sample are given in Fig. 1. From the X-ray power data refinements, the crystal of $Na_8(SiAlO_4)_6(OH)_2\cdot 2H_2O$ as first studied by Hassan and Grundy [3] could be confirmed (ICSD-No. 36050). The peaks could be indexed indicating no obvious contribution of crystalline impurity phase. The refined cubic cell parameter α is 8.890 Å, all of the Na, Si, Al atoms and the O atoms involved in silica tetrahedrons and alumina tetrahedrons have the established positions with the full occupancy, and Si–O, Al–O bonds are 1.616, 1.743 Å, respectively. While the O atoms in Refs. $(OH)^-$ and H_2O groups have uncertain positions, almost having 24 possible sites with the occupancy of 0.167. The small hydrogen atoms may not be determined experimentally.

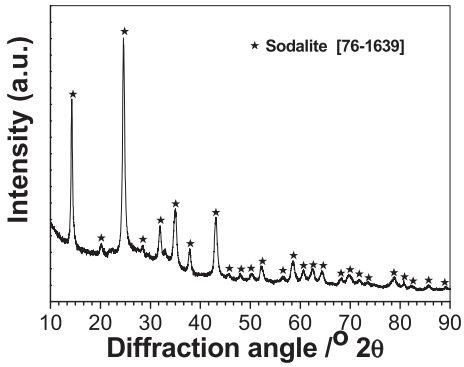

Fig. 1. X-ray power diffraction pattern of the sample, the Bragg reflex positions of $Na_8(SiAlO_4)_6(OH)_2\cdot 2H_2O$ are marked.

The UV–Vis absorption spectra and first derivative absorption spectra of the sample are depicted in Fig. 2. It is observed that the spectra reveal one obvious adsorption peak located at (269.9 ± 0.2) nm. A small adsorption peak labeled at (209.0 ± 0.2) nm is not obvious in Fig. 2a, but easily recognized in Fig. 2b. As shown in Fig. 2c, the diffuse reflectance spectra of the sample was also measured to check these two peak values. The fluctuations in range of the visible light may be related with the negligible amorphous impurities and instrument noise. The photon energy may be expressed as below, $E_{phot} = (1239/\lambda)$ eV, whereλ is the wavelength in nanometers. By this means, the photon energy is calculated to be (4.59 ± 0.01) and (5.93 ± 0.01) eV for absorption spectra, respectively, adjacent to the results of (4.66 ± 0.01) and (6.07 ± 0.01) eV by reflectance spectra measurements. It is noted that the photon band gap of the sample should not be obtained from the extrapolation of the adsorption edge onto the energy axis because of the multiple-peaked feature. There is another method for band gap from adsorption spectra by calculating the first derivative of absorbance with respect to the photon energy and finding the maxima at the lower energy sides [38–41]. So the photon band gap should be (4.53 ± 0.01) eV and the other peak corresponds to (5.96 ± 0.01) eV shown in Fig. 2b. In summary, the photon band gap should be in range of 4.5 eV–4.7 eV combining the results of the absorption spectra and reflectance spectra.

Overall, we have confirmed the chemical formula and determined the photon band gap of our sample. In next section, the configurations of sodalite were constructed and calculated by VASP, and then the electronic properties of sodalite were compared with experimental values.

3.2. The structure and electronic properties the sodalite

The side view of the origin structure of sodalite $Na_8(SiAlO_4)_6(OH)_2\cdot 2H_2O$ is shown on the left side of Fig. 3. The positions are defined experimentally except the $(OH)^-$ and H_2O, there are two cages in unit cell: a full cage and one-eighth of the eight nearest neighbor cage. Based on the distance, the twelve oxygen possible occupancy positions in each cage may be regarded as four effective positions in formation of tetrahedral structure. Two of effective positions should be selected and given $(OH)^-$ or H_2O groups. As shown in Fig. 3, the central oxygen tetrahedral is marked in red circle and the nearest neighbors in blue, and the scheme of the $(OH)^-$ and H_2O groups distribution by two oxygen tetrahedrons is depicted in the upper of middle. For simplicity, an arrow line is adopted to stand for one arrangement of $(OH)^-$ and H_2O groups, i.e. $(OH)^-$ near to arrow head and H_2O group close to narrow tail. There are seven possible configurations according to the symmetry. The